# Magnetorotational Instability

Edgar Knobloch

University of California, Berkeley, CA 94720, USA
IMFT - INPT - UPS Chaire Pierre de Fermat de la région Midi-Pyrénées

Banff, 8 November 2012
Joint work with Keith Julien, CU Boulder

# Talk Outline

- Motivation
  - Accretion disks
  - Laboratory experiments
- Ideal MRI
- Numerical simulations
  - Local shearing box approximation
  - Global simulations
  - Importance of dissipative processes
- Theory
  - Scaling of the equations
  - Asymptotics
  - Sample solutions in two different cases
  - Predictions of the saturated state of the MRI
  - Generalizations
- Prospects

# Motivation

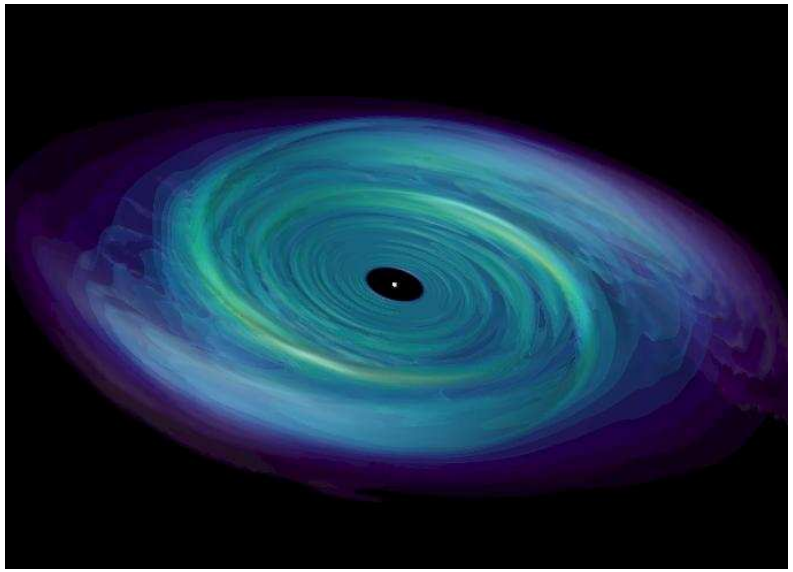

- Turbulent accretion disks require the presence of an efficient mechanism for angular momentum transport
- Many mechanisms have been investigated and found wanting
  - Shear instabilities
  - Barotropic instabilities (Dubrulle et al)
  - Baroclinic instabilities (Knobloch, Spruit)
  - Sound waves (Glatzel, Kaisig)
  - Shock waves (Spruit)
  - Finite amplitude instabilities (Dubrulle, Longaretti, Zahn)

# Motivation

- Magnetic field-induced instabilities appear most promising
- Magnetorotational instability has several appealing properties (Balbus and Hawley 1991, 1998)
  - It is a linear instability
  - It is triggered by weak poloidal magnetic field
  - It is axisymmetric
  - It occurs in Rayleigh-stable regime when the angular velocity decreases radially
  - It grows on a dynamical timescale
  - It is fundamentally a local instability
- Efficiency of angular momentum transport depends on the saturation of the MRI
- Central question: how does the MRI saturate?
  This is a **nonlinear** problem!
- Is the saturated state perhaps a dynamo? Lesur and Ogilvie (2008)

# Ideal MRI

The basic equations are

$$\rho\left[\frac{\partial \mathbf{u}}{\partial t} + (\mathbf{u}\cdot\nabla)\mathbf{u}\right] = -\nabla p - \frac{1}{2\mu_0}\nabla B^2 + \frac{1}{\mu_0}(\mathbf{B}\cdot\nabla)\mathbf{B},$$

$$\frac{\partial \mathbf{B}}{\partial t} + (\mathbf{u}\cdot\nabla)\mathbf{B} = (\mathbf{B}\cdot\nabla)\mathbf{u},$$

$$\nabla\cdot\mathbf{u} = \nabla\cdot\mathbf{B} = 0.$$

These equations have a basic axisymmetric solution of the form

$$\mathbf{u_0} = [0, V(r), 0], \qquad \mathbf{B_0} = [0, B_\phi(r), B_z(r)]$$

in $(r, \phi, z)$ coordinates.

# Ideal MRI: eigenvalue relation

We look at **axisymmetric** perturbations of the form $f(r,\phi,z,t) = f(r)\exp i(nz+\omega t)$. For given basic state and $n$ the (complex) frequency $\omega$ is an eigenvalue of the problem (Acheson 1973)

$$\frac{d}{dr}\left[(\omega^2 - n^2 V_z^2)\left(\frac{du}{dr}+\frac{u}{r}\right)\right] - n^2\left[\omega^2 - n^2 V_z^2 + r\frac{d}{dr}\left(\frac{V_\phi^2}{r^2}-\frac{V^2}{r^2}\right)\right]u$$
$$= -\frac{4n^2}{r^2}\frac{(nV_\phi V_z + \omega V)^2}{(\omega^2 - n^2 V_z^2)}u,$$

where

$$V_\phi^2 = \frac{B_\phi^2}{\mu_0\rho}, \qquad V_z^2 = \frac{B_z^2}{\mu_0\rho}.$$

The azimuthal magnetic field plays an important role

- the gradient $d(V_\phi^2/r^2)/dr$ competes with $d(V^2/r^2)/dr$
- prevents the problem from being an eigenvalue problem for $\omega^2$ alone

# Ideal MRI: the boundary conditions $u(a) = u(b) = 0$

Case (i) $V_z = \mathrm{const} \neq 0$, $V_\phi = 0$. Multiplying by $u^*$ and integrating over $a \leq r \leq b$ yields a quadratic equation for $\omega^2$:

$$(\omega^2 - n^2 V_z^2)^2 = \frac{n^2}{D} \int_a^b \left[ \frac{\omega^2}{r^2} \frac{d}{dr} r^2 V^2 - r^2 n^2 V_z^2 \frac{d}{dr} \left( \frac{V^2}{r^2} \right) \right] |u|^2 \, dr,$$

where

$$D \equiv \int_a^b \left( r \left| \frac{du}{dr} \right|^2 + \frac{|u|^2}{r} + n^2 r |u|^2 \right) dr > 0.$$

Thus if the disk is hydrodynamically stable ($d(r^2 V^2)/dr > 0$)

- sufficient condition for stability is that $d(V^2/r^2)/dr > 0$ in $a < r < b$
- necessary condition for instability is that $d(V^2/r^2)/dr < 0$ somewhere in $a < r < b$

This is the classical MRI of Velikhov (1959) and Chandrasekhar (1960); see also Acheson (1973), Acheson and Hide (1973), Balbus and Hawley (1991), Knobloch (1992).

# Ideal MRI: general properties of the eigenvalue relation

Case (ii) $V_z = \mathrm{const} \neq 0$, $V_\phi \neq 0$. In this case

$$\frac{d}{dr} r \frac{du}{dr} - \frac{u}{r} - n^2 r u =$$
$$\frac{n^2}{(\omega^2 - n^2 V_z^2)^2} \left[ r^2 \frac{d}{dr} \left( \frac{V_\phi^2 - V^2}{r^2} \right) (\omega^2 - n^2 V_z^2) - \frac{4}{r} (n V_\phi V_z + \omega V)^2 \right] u.$$

For unstable, exponentially growing modes ($\omega = -i\lambda$, $\lambda > 0$) we obtain

$$(\lambda^2 + n^2 V_z^2)^2 = \frac{n^2}{D} \int_a^b \left[ r^2 \frac{d}{dr} \left( \frac{V_\phi^2 - V^2}{r^2} \right) (\lambda^2 + n^2 V_z^2) + \frac{4}{r} (n V_\phi V_z - i\lambda V)^2 \right] |u|^2$$

It follows that

- a necessary condition for an exponential instability is

$$\int_a^b \frac{1}{r} V_\phi V |u|^2 \, dr = 0,$$

  i.e., $V_\phi$ or $V$ (or both) must change sign somewhere in $a < r < b$. Thus this kind of instability is not to be expected.

# Ideal MRI: Case (ii) ctd

Instead we find

- exponentially growing oscillations (overstability, or Hopf bifurcation)
- this is because the magnetic helicity in the basic state breaks the reflection symmetry $z \to -z$ (Knobloch 1992, 1996)
- generic bifurcation with the resulting SO(2) symmetry is a Hopf bifurcation to traveling waves (eg. Ecke et al 1992)
- these TW have recently been observed in the PROMISE experiment (Stefani et al 2006, 2007)

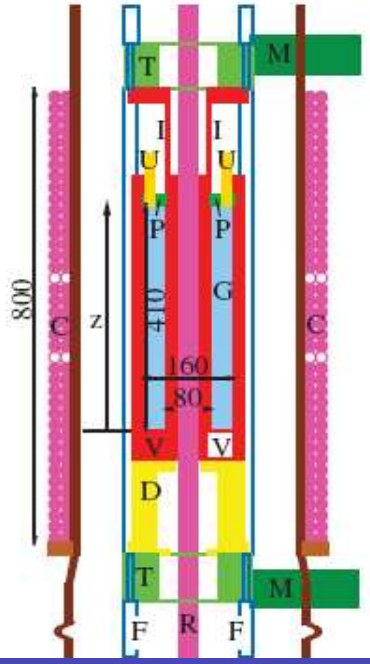


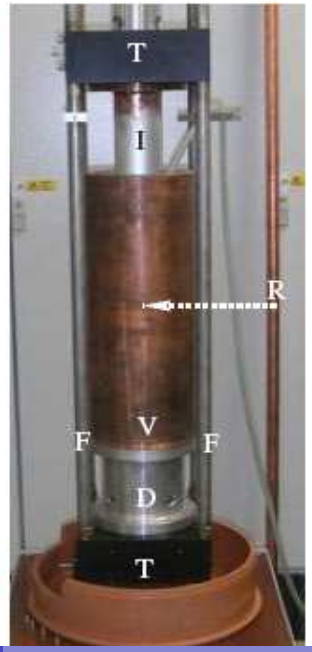


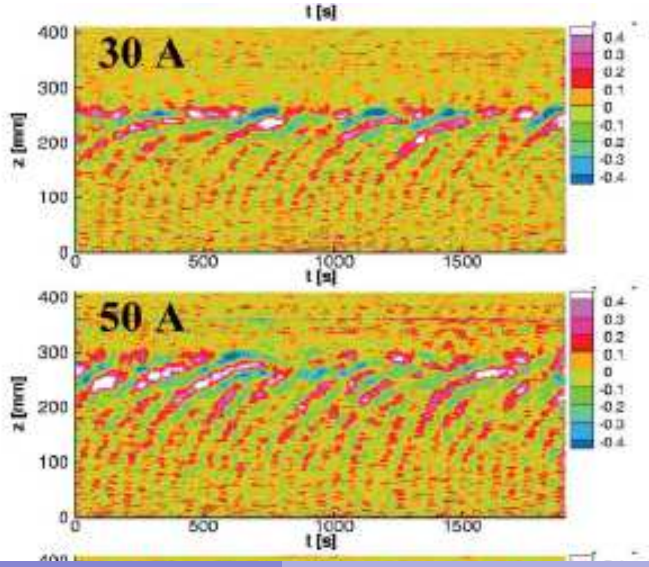

# Ideal MRI: convective vs absolute instability

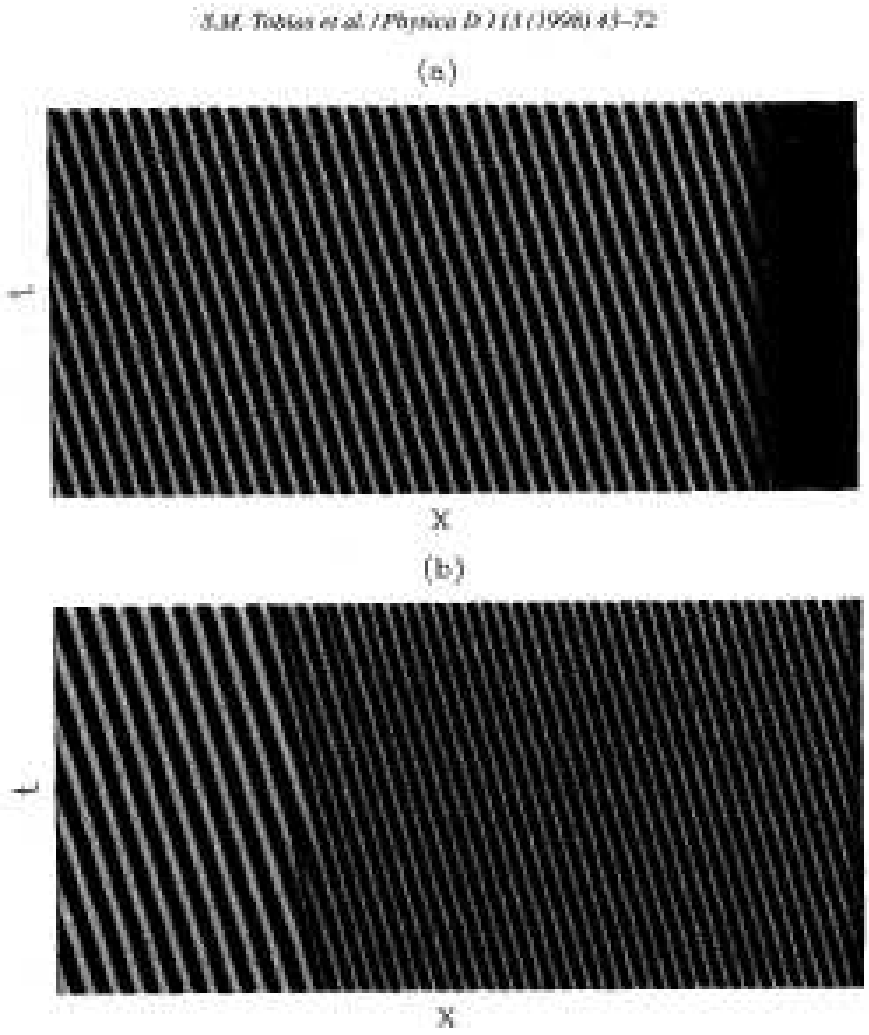


Dynamo waves traveling towards the equator (Tobias et al 1997, 1998)

# Numerical simulations: shearing box geometry

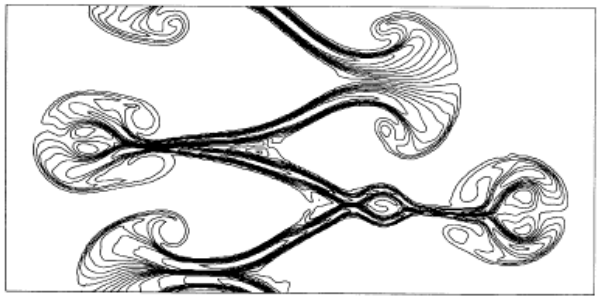

FIG. 5b

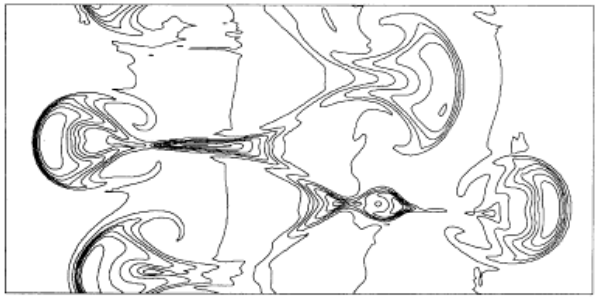

FIG. 5c

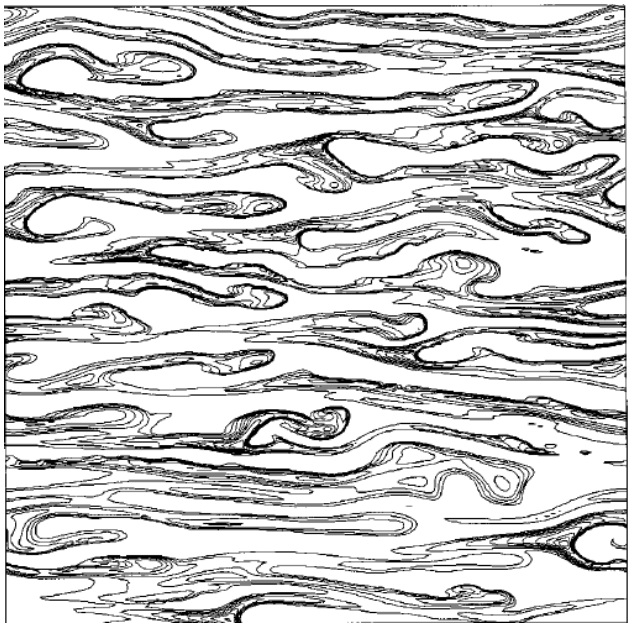

- Balbus-Hawley 1991a,b: Thin sheets of matter moving radially inwards and outwards
- X-points suggest reconnection process important to saturation
- Goodman & Xu 1994, Pessah & Goodman 2009: shear instabilities of the interpenetrating sheets
- Sano et al 1998: whether saturation occurs depends on the Elsasser number $\Lambda \equiv v_A^2/\eta\Omega$

# Numerical simulations

- Sano et al: compressible flow in shearing box geometry



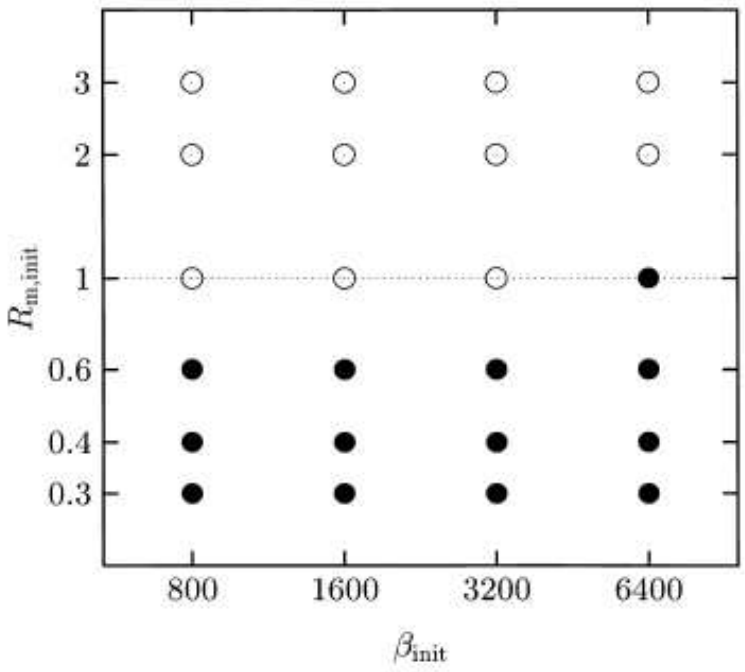


FIG. 1.—Final state for calculated disk models. Filled circles denote the models in which the saturated state continues at least for 100 orbits. The models ended by the channel solution are shown by open circles.

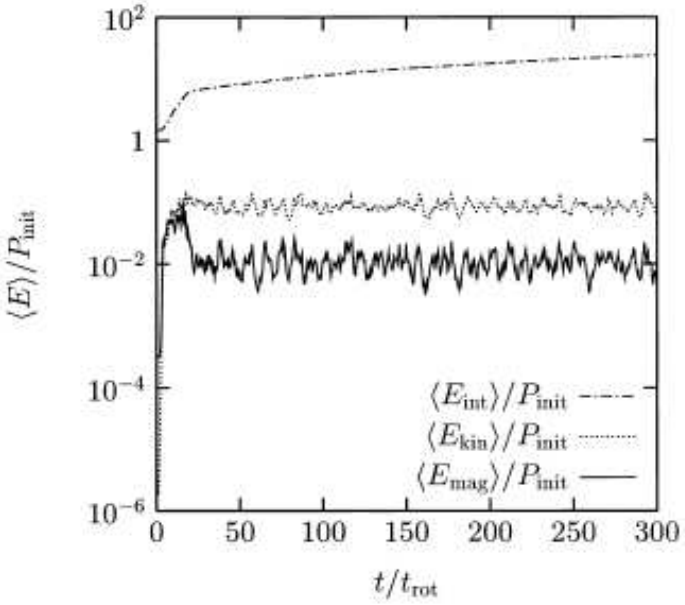


FIG. 2.—Time evolutions of volume-averaged internal (thermal) energy, perturbed kinetic energy, and magnetic energy for the saturated model ($\beta_{init} = 3200$, $R_{m,init} = 0.6$). Here the perturbed kinetic energy is defined as $E_{kin} = \rho(v_x^2 + \delta v_y^2 + v_z^2)/2$. These values are given in terms of the initial gas pressure $P_{init}$.

- Global geometry: Kersalé et al 2004, 2006; Cattaneo et al (still eagerly awaited!)

# Numerical simulations

Fromang and Papaloizou (2007):

- Investigated numerical diffusion of both velocity and magnetic fields in a shearing box with zero net flux using ideal MHD and ZEUS: $Pm \equiv \nu_{\rm num}/\eta_{\rm num} > 1$
- Found that rate of angular momentum transport $\alpha$ declined as resolution was increased
- Concluded that it is important (!) to explicitly include resolved physical dissipation

Fromang et al (2007):

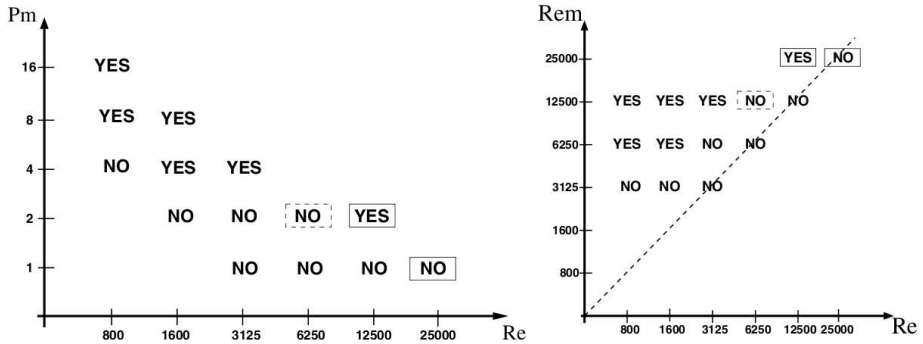


**Fig. 11.** Summary of the state (turbulent or not) of the flow in an (Re, Pm) plane (left panel) and in an (Re, $\mathrm{Re_M}$) plane (right panel) for the models presented in this paper. In the later, the dashed line represents the Pm = 1 case. On both panels, "YES" means that a non vanishing transport coefficient $\alpha$ was measure while "NO" means that MHD turbulence eventually decays: $\alpha = 0$. All cases use a resolution $(N_x, N_y, N_z) = (128, 200, 128)$, except the models appearing in a solid squared box, for which the resolution was doubled. The model appearing in a dashed line squared box corresponds to the marginal model described in Fig. 7.

- Constant $Re$: angular momentum transport increases with $Pm$

# Formulation of a Model Problem: Knobloch & Julien 2005

- Shearing box approximation at $r^*$ with local angular velocity $\Omega^*(r^*)\hat{\mathbf{z}}$:
- Straight channel: $-L^*/2 \leq x^* \leq L^*/2$, $-\infty < y^* < \infty$, $-\infty < z^* < \infty$
- Linear shear: $\mathbf{U_0}^* = (0, \sigma^* x^*, 0)$
- Constant B-Field: $\mathbf{B_0}^* = (0, B^*_{tor}, B^*_{pol})$
- Perturb: $\mathbf{u} \equiv (u, v, w) = (-\psi_z, v, \psi_x)$, $\mathbf{b} \equiv (a, b, c) = (-\phi_z, b, \phi_x)$

Axisymmetric Equations

$$\nabla^2\psi_t + 2\Omega v_z + J(\psi, \nabla^2\psi) = v_A^2\nabla^2\phi_z + v_A^2 J(\phi, \nabla^2\phi) + \nu\nabla^4\psi, \quad (1)$$

$$v_t - (2\Omega + \sigma)\psi_z + J(\psi, v) = v_A^2 b_z + v_A^2 J(\phi, b) + \nu\nabla^2 v, \quad (2)$$

$$\phi_t + J(\psi, \phi) = \psi_z + \eta\nabla^2\phi, \quad (3)$$

$$b_t + J(\psi, b) = v_z - \sigma\phi_z + J(\phi, v) + \eta\nabla^2 b, \quad (4)$$

where $J(f, g) \equiv f_x g_z - f_z g_x$.

- $v_A \equiv B^*_{pol}/\sqrt{\mu_0\rho^*}U^*$, $\Omega$, $\nu$, $\eta$ are the *dimensionless* Alfvén speed, rotation rate, kinematic viscosity and ohmic diffusivity

# Remarks on the Model Problem

Local shearing box approx'n $\Rightarrow$ special properties of model eqs:

- Toroidal field $B^*_{tor}$ drops out
  - suppression of hoop stresses
  - toroidal field remains in the radial pressure balance

$$2\Omega^* V_0^* + \frac{V_0^{*2}}{r^*} = \frac{1}{\rho^*}\frac{dP_0^*}{dr^*} + \frac{d}{dr^*}\left(\frac{B_{tor}^{*2}}{2\mu_0\rho^*}\right) + \frac{B_{tor}^{*2}}{\mu_0\rho^* r^*} \tag{5}$$

- no distinction between inward and outward directions
  - symmetry $x \to -x$, $(\psi, v, \phi, b) \to -(\psi, v, \phi, b)$
- MRI is an exponentially growing instability
  - this is not the case in polar coordinates with nonzero $B^*_{tor}$

# Linear Theory

- Linearization about the trivial state $\psi = v = \phi = b = 0$:
- Perturbation $\exp[\lambda t + ikx + inz]$, $p = k^2 + n^2 \Rightarrow$ dispersion relation

$$p[(\lambda+\nu p)(\lambda+\eta p)+v_A^2 n^2]^2+2\Omega n^2[(\lambda+\eta p)^2(2\Omega+\sigma)+\sigma v_A^2 n^2] = 0. \quad (6)$$

- Conventional view of MRI: positive growth rate $\lambda$ achieved for sufficiently large vertical wavenumbers $n$ whenever $\sigma < 0$, $v_A \neq 0$, provided only that $\nu$ and $\eta$ are sufficiently small
  - For $\nu = \eta = 0$

$$\lambda^2 = -\frac{v_A^2 n^2 \sigma}{2\Omega + \sigma} + O(v_A^4 n^4). \quad (7)$$

  - For $\lambda = 0$ threshold for instability exists. For small $\nu, \eta$ critical Elsasser number

$$\Lambda_c \equiv v_A^2/\Omega\eta = -\eta\left(\frac{2\Omega + \sigma}{\Omega\sigma}\right)\frac{p^2}{n^2} + O(\nu, \eta)^3. \quad (8)$$

  - Reconnection effects described by finite $\eta$ are more important for stabilizing the system against the MRI than viscosity.

# Scaling Assumptions

- Traditional approach to nonlinear saturation: weakly nonlinear theory with $(\Lambda - \Lambda_c)/\Lambda_c \ll 1$ (eg. Umurhan & Regev 2007)
- Our approach: strongly nonlinear theory
  - shear is the dominant source of energy for the MRI
  - MRI itself requires the presence of a (weaker) vertical magnetic field
  - dissipative effects are weaker still but cannot be ignored since they are ultimately responsible for the saturation of the instability
- Hence scaling:
  - rapid rotation, strong shear: $(\Omega, \sigma) = \epsilon^{-1}(\hat{\Omega}, \hat{\sigma})$
  - magnetic field: $v_A = 1$ i.e. , $U^* = v_A^* \equiv B^*_{pol}/\sqrt{\mu_0 \rho^*}$
  - weak dissipative processes: $(\nu, \eta) = \epsilon(\hat{\nu}, \hat{\eta})$
  - thin fingers, strong growth: $\partial_x \to \partial_x, \quad \partial_z \to \epsilon^{-1}\partial_z, \quad \partial_t \to \epsilon^{-1}\partial_t$
- In the following we take $\epsilon \ll 1$, or equivalently $Rm \gg S \gg \max(1, Pm)$, while $\Lambda = O(1)$. Here $Rm = |\sigma^*| L^{*2}/\eta^* = O(\epsilon^{-2})$, $Pm = \nu^*/\eta^* = O(1)$, $S \equiv v_A^* L^*/\eta^* = O(\epsilon^{-1})$ are the magnetic Reynolds, magnetic Prandtl and Lundquist numbers.

# Scaled Equations

- In parallel with the above assumptions we need to make further assumptions about the relative magnitude of the various fields:
- we find $(\psi, \phi) \to \epsilon(\psi, \phi)$, $(v, b) \to \epsilon^{-1}(v, b)$ leads to a self-consistent set of reduced pdes
- scaled pdes:

$$\epsilon \frac{D}{Dt}\left(\partial_x^2 + \epsilon^{-2}\partial_z^2\right)\psi + 2\epsilon^{-3}\hat{\Omega} v_z = v_A^2\left(\partial_x^2 + \epsilon^{-2}\partial_z^2\right)\phi_z + \epsilon v_A^2 J\left(\phi, \left(\partial_x^2 + \epsilon^{-2}\partial_z^2\right)\phi\right) + \epsilon^2 \hat{\nu}\left(\partial_x^2 + \epsilon^{-2}\partial_z^2\right)^2 \psi \tag{9}$$

$$\epsilon^{-1}\frac{D}{Dt} v - \epsilon^{-1}(2\hat{\Omega} + \hat{\sigma})\psi_z = \epsilon^{-2} v_A^2 b_z + \epsilon^{-1} v_A^2 J(\phi, b) + \hat{\nu}(\partial_x^2 + \epsilon^{-2}\partial_z^2) v \tag{10}$$

$$\epsilon \frac{D}{Dt}\phi = \psi_z + \epsilon^2 \hat{\eta}(\partial_x^2 + \epsilon^{-2}\partial_z^2)\phi \tag{11}$$

$$\epsilon^{-1}\frac{D}{Dt} b = \epsilon^{-2} v_z - \epsilon^{-1}\hat{\sigma}\phi_z + \epsilon^{-1} J(\phi, v) + \hat{\eta}(\partial_x^2 + \epsilon^{-2}\partial_z^2) b, \tag{12}$$

where $D/Dt = \partial_t + J[\psi, \bullet]$.

# Derivation of Reduced PDEs

- To solve the scaled equations we suppose $\psi(x,z,t) = \psi_0(x,z,t) + \epsilon\psi_1(x,z,t) + \ldots$, etc.
- Deduction: Leading order azimuthal fields $v_0, b_0$ represent large-scale adjustment to background shear and toroidal field due to MRI
  - From Eqs for azimuthal fields $v, b$ at $O(\epsilon^{-2})$ and poloidal fields $\psi$ at $O(\epsilon^{-3})$

$$v_A^2 b_{0z} + \hat{\nu} v_{0zz} = 0, \qquad v_{0z} + \hat{\eta} b_{0zz} = 0, \qquad 2\widehat{\Omega} v_{0z} = 0 \tag{13}$$

  - Hence

$$v_0 = V(x,t), \qquad b_0 = B(x,t) \tag{14}$$

  - Averaging in $t$ at $O(\epsilon^{-1}) \Rightarrow$ slow time evolution. Hence

$$v_0 = V(x), \qquad b_0 = B(x) \tag{15}$$

# Derivation of Reduced PDEs, cont'd

- From Eqs for azimuthal fields $v, b$ at $O(\epsilon^{-1})$ and poloidal fields $\psi, \phi$ at $O(\epsilon^{-2})$, $O(1)$

$$\psi_{0zzt} + 2\widehat{\Omega} v_{1z} = v_A^2 \phi_{0zzz} + \widehat{\nu} \psi_{0zzzz} \tag{16}$$

$$v_{1t} - (2\widehat{\Omega} + \widehat{\sigma} + V'(x))\psi_{0z} = v_A^2 b_{1z} - v_A^2 B'(x)\phi_{0z} + \widehat{\nu} v_{1zz} \tag{17}$$

$$\phi_{0t} = \psi_{0z} + \widehat{\eta}\phi_{0zz} \tag{18}$$

$$b_{1t} - B'(x)\psi_{0z} = v_{1z} - (\widehat{\sigma} + V'(x))\phi_{0z} + \widehat{\eta} b_{1zz} \tag{19}$$

- Closure requires determination of $V'(x), B'(x)$.
  - Averaging Eqs for azimuthal fields $v, b$ at $O(1)$ in $z, t$ and integrating gives

$$\widehat{\nu} V'(x) = \overline{\psi_0 v_{1z}} - v_A^2 \overline{\phi_0 b_{1z}} + C_1 \tag{20}$$

$$\widehat{\eta} B'(x) = \overline{\psi_0 b_{1z}} - \overline{\phi_0 v_{1z}} + C_2 \tag{21}$$

- $C_1$ is determined by BC's; $0 < C_2 < C_{max}$ range of total to zero support of disk by radial pressure gradient.

# Strongly Nonlinear Single-Mode Solutions

These equations have stationary solutions of the form

$$\psi_0 = \frac{1}{2}(\Psi(x)\, e^{inz} + \text{c.c.}), \quad v_1 = \frac{1}{2}(\mathcal{V}(x)\, e^{inz} + \text{c.c.}), \tag{22}$$
$$\phi_0 = \frac{1}{2}(\mathcal{F}(x)\, e^{inz} + \text{c.c.}), \quad b_1 = \frac{1}{2}(\mathcal{B}(x)\, e^{inz} + \text{c.c.}),$$

where

$$\mathcal{F} = \frac{i\Psi}{\hat{\eta} n}, \tag{23}$$

$$\mathcal{V} = \frac{(v_A^2 + \hat{\eta}^2 n^2)V' + \hat{\eta}^2 n^2(2\hat{\Omega} + \hat{\sigma}) + v_A^2 \hat{\sigma}}{n\hat{\eta}(v_A^2 + \hat{\nu}\hat{\eta} n^2)}\, i\Psi, \tag{24}$$

$$\mathcal{B} = \frac{i(v_A^2 + \hat{\nu}\hat{\eta} n^2)B' + n(\hat{\nu}(\hat{\sigma} + V') - \hat{\eta}(2\hat{\Omega} + \hat{\sigma} + V'))}{n\hat{\eta}(v_A^2 + \hat{\nu}\hat{\eta} n^2)}\Psi, \tag{25}$$

and we obtain the nonlinear dispersion relation

$$2\hat{\Omega}[(v_A^2 + \hat{\eta}^2 n^2)V' + (2\hat{\Omega} + \hat{\sigma})\hat{\eta}^2 n^2 + \hat{\sigma} v_A^2] + n^2(v_A^2 + \hat{\nu}\hat{\eta} n^2)^2 = 0. \tag{26}$$

- Except for the presence of the additional shear rate $V'$ this is nothing but the linear dispersion relation for the MRI in our scaling regime

# Nonlinear Dispersion Relation

- For each wavenumber $n$ the dispersion relation determines $V'$

$$2\hat{\Omega}[(v_A^2 + \hat{\eta}^2 n^2)V' + (2\hat{\Omega} + \hat{\sigma})\hat{\eta}^2 n^2 + \hat{\sigma} v_A^2] + n^2(v_A^2 + \hat{\nu}\hat{\eta} n^2)^2 = 0$$

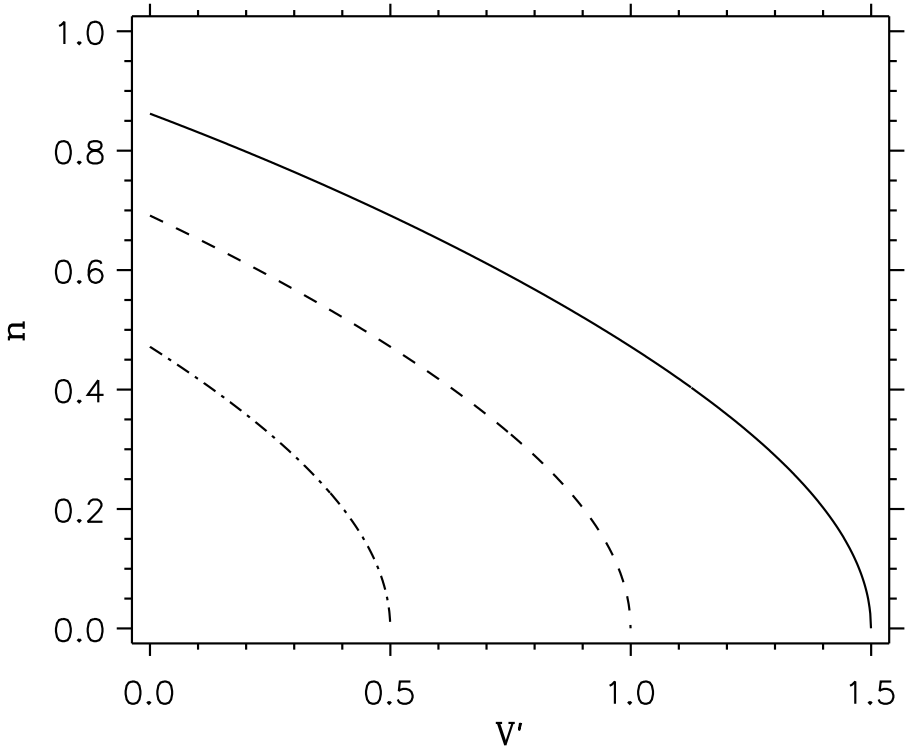


Parameters: $\widehat{\Omega} = 1, v_A = 1, \widehat{\nu} = \widehat{\eta} = 1$, and $\widehat{\sigma} = -1.5, -1, -0.5$ (solid, dashed, dashed-dot).

The decrease in $n$ with increasing $V'$ indicates coarsening as the MRI saturates.

# Single-Mode Solutions: Closure

- Closure requires the determination of $V', B'$ as a function of $\Psi$. Since

$$\psi_0 = \frac{1}{2}(\Psi(x)\, e^{inz} + \text{c.c.}), \quad v_1 = \frac{1}{2}(\mathcal{V}(x)\, e^{inz} + \text{c.c.}), \tag{27}$$
$$\phi_0 = \frac{1}{2}(\mathcal{F}(x)\, e^{inz} + \text{c.c.}), \quad b_1 = \frac{1}{2}(\mathcal{B}(x)\, e^{inz} + \text{c.c.}),$$

we find

$$V'(x) = \frac{C_1 - \frac{1}{2}\beta|\Psi|^2}{\widehat{\nu} + \frac{1}{2}\alpha|\Psi|^2}, \qquad B'(x) = \frac{\widehat{\eta} C_2}{\widehat{\eta}^2 + \frac{1}{2}|\Psi|^2}. \tag{28}$$

$$\alpha = \frac{\widehat{\nu} v_A^2 + \widehat{\eta}^3 n^2}{\widehat{\eta}^2(v_A^2 + \widehat{\nu}\widehat{\eta} n^2)}, \qquad \beta = \frac{(2\widehat{\Omega} + \widehat{\sigma})\widehat{\eta}^3 n^2 + v_A^2(\widehat{\sigma}\widehat{\nu} - 2\widehat{\Omega}\widehat{\eta})}{\widehat{\eta}^2(v_A^2 + \widehat{\nu}\widehat{\eta} n^2)}. \tag{29}$$

- MRI requires $C_1 = 0$ for nonzero $V'$ and $\Psi$
- Nonlinear dispersion relation then gives the saturated value of $|\Psi|$:

$$|\Psi|^2 = -\frac{2\widehat{\nu}\widehat{\eta}^2\left[n^2(v_A^2 + \widehat{\nu}\widehat{\eta} n^2)^2 + 2\widehat{\Omega}\widehat{\sigma} v_A^2 + 2\widehat{\Omega}(2\widehat{\Omega} + \widehat{\sigma})\widehat{\eta}^2 n^2\right]}{\left[4\widehat{\Omega}^2 v_A^2 \widehat{\eta} + n^2\left(v_A^2 + \widehat{\nu}\widehat{\eta} n^2\right)\left(\widehat{\nu} v_A^2 + \widehat{\eta}^3 n^2\right)\right]} \tag{30}$$

This bifurcation equation determines the saturation amplitude

# Single Mode Results I

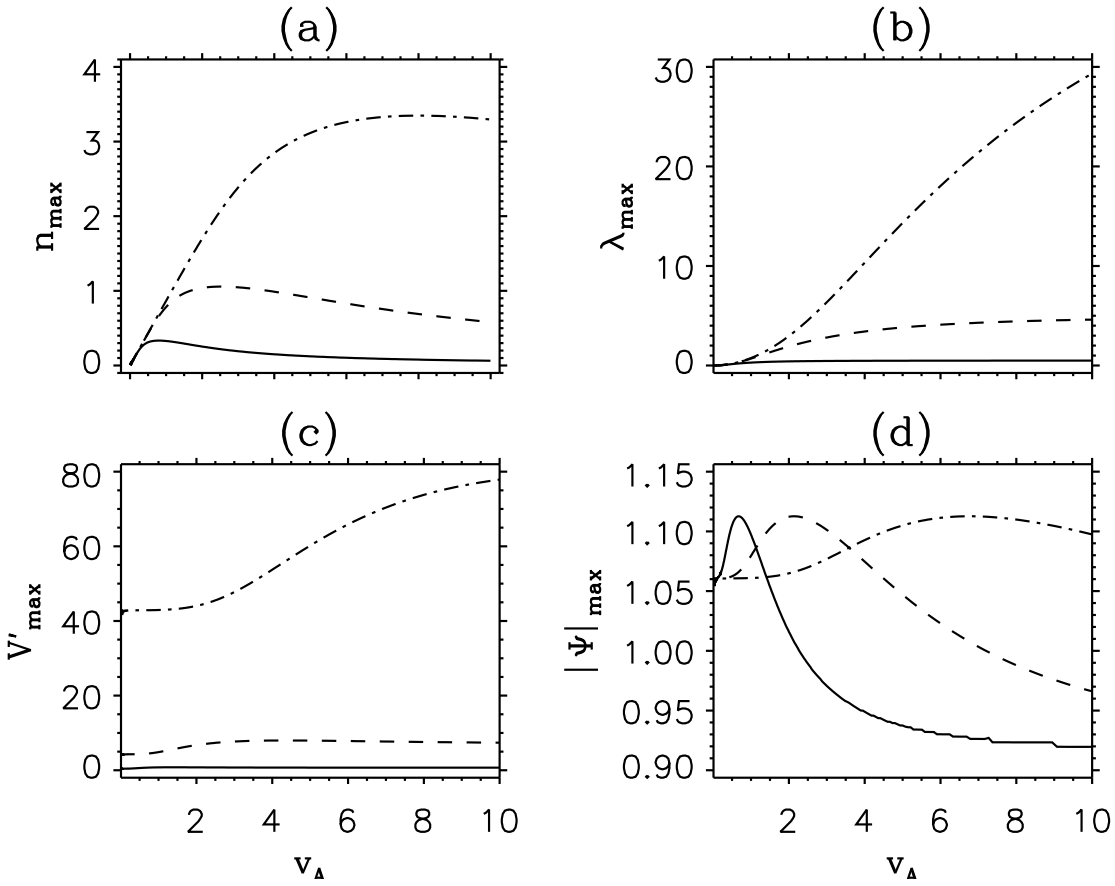


Parameters: $\widehat{\Omega} = -2\widehat{\sigma}/3$, $\widehat{\nu} = \widehat{\eta} = 1$, and $\widehat{\sigma} = -100, -10, -1$ (dashed-dot, dashed, solid)

- Maximum growth rate $\lambda$ and $V'$ increases with $v_A$, whereas associated wavenumber $n$ and saturation level $|\Psi|$ peaks
- Increasing $n$ initially gets around stabilizing Lorentz force but once MRI flow is capable of slipping through the field further increase in $n$ is of no benefit

# Single Mode Results II

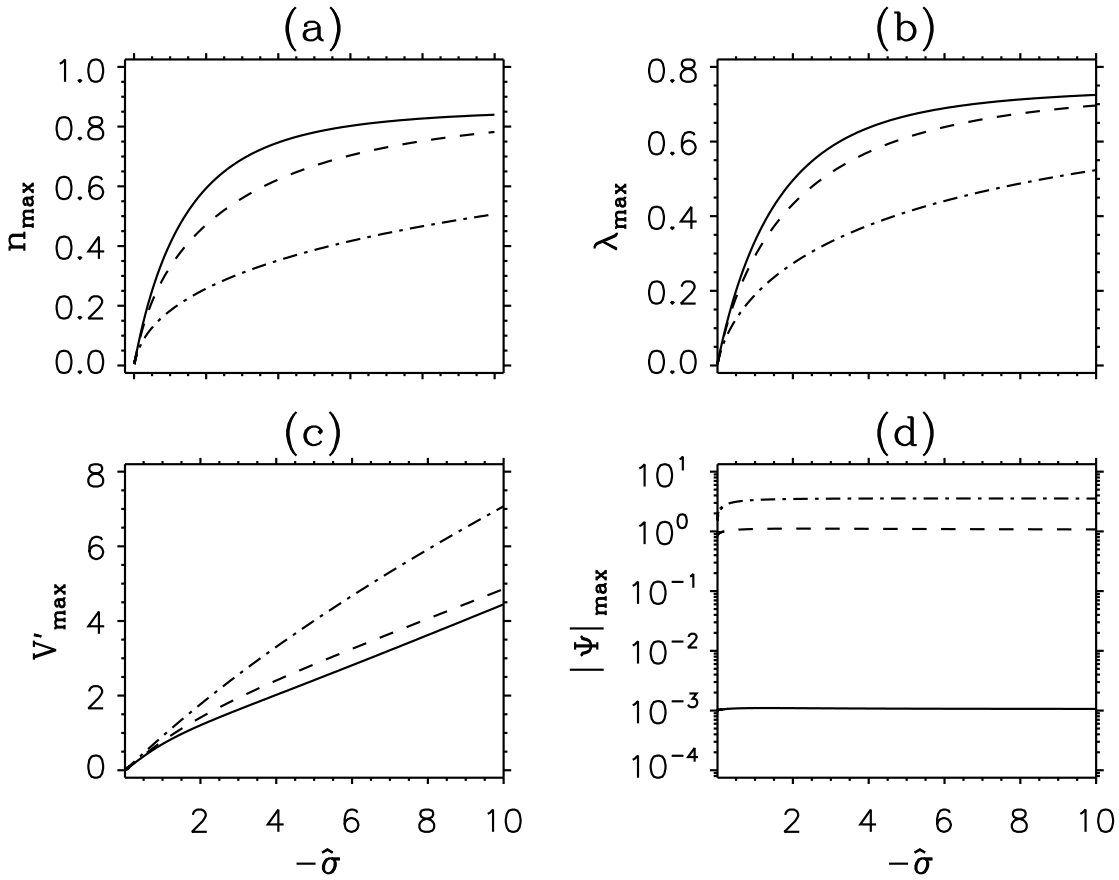


Parameters: $\widehat{\Omega} = -2\widehat{\sigma}/3$, $v_A = \widehat{\eta} = 1$, and $\widehat{\nu} = 10^{-6}, 1, 10$ (solid, dashed, dashed-dot)

- $V'$ increases rapidly with shear rate $|\widehat{\sigma}|$ while $n, \lambda, |\Psi|$ saturate. This is a consequence of the reduced role of the Coriolis force
- Saturation values increase with $\widehat{\nu}$ indicating subtle role of viscosity in nonlinear regime: larger viscosity transports more ang. mtm., competing with magnetic stresses

# Single Mode Results III

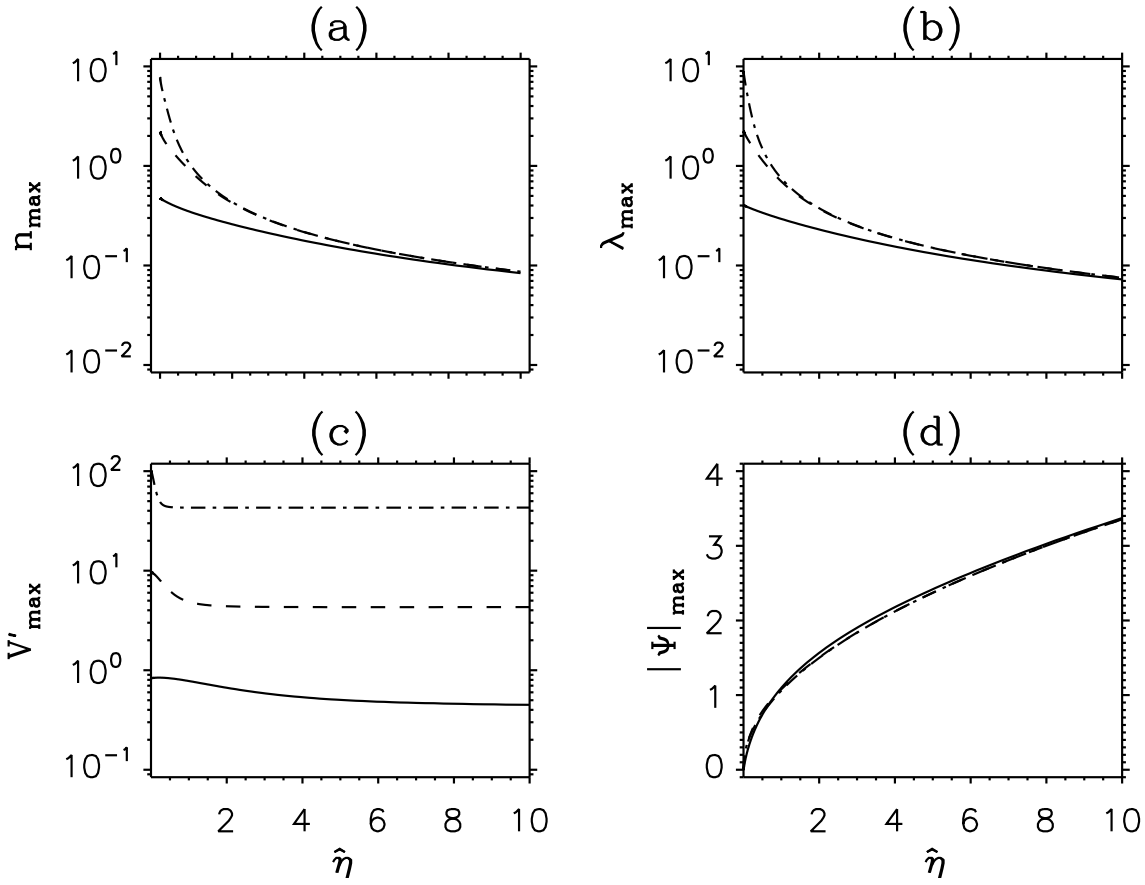


Parameters: $\widehat{\Omega} = -2\widehat{\sigma}/3$, $v_A = \widehat{\nu} = 1$, and $\widehat{\sigma} = -100, -10, -1$ (dashed-dot, dashed, solid)

- For small $\widehat{\eta}, \widehat{\nu}$ MRI grows on the dynamical timescale. As $\widehat{\eta}$ increases growth rate and wavenumber decrease but saturation level of $|\Psi|$ increases
- Behavior consistent with the idea that reconnection reduces the effect of Lorentz force and thus enhances the amplitude of MRI. This does not translate into increased $V'$ (i.e. modification of background shear)

# Approach to Saturated State

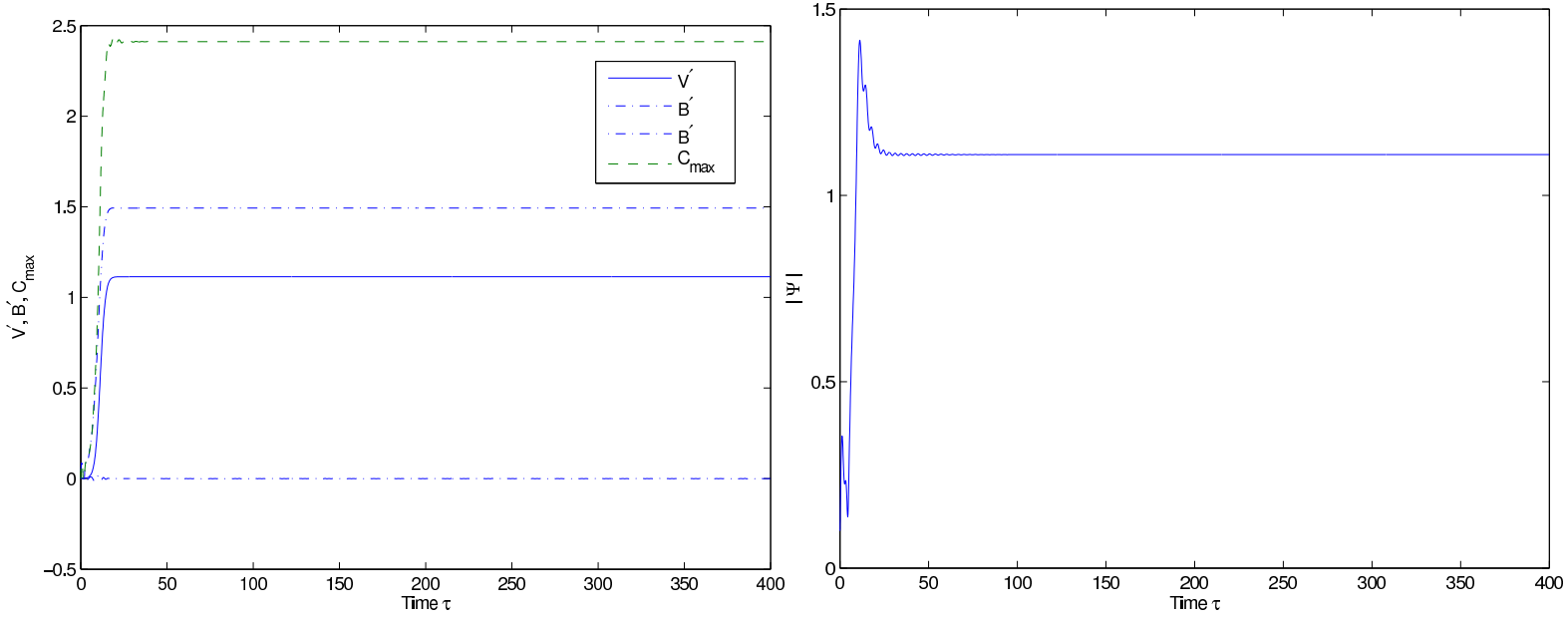


- Time-dependent evolution of an x-invariant single-mode perturbation indicates approach to predicted stationary solution
- Above results display extreme cases: disks supported entirely by mechanical ($B' = 0$) or magnetic ($B' \neq 0$) pressure
- $\nu_t = 2\pi\epsilon|\Psi| \sim O(\epsilon)$: turbulent viscosity associated with developed MRI

# A different scaling

If we now suppose that

$$(\nu, \eta) = \epsilon(\widehat{\nu}, \widehat{\eta}), \quad (\Omega, \sigma) = \delta^{-1}(\widehat{\Omega}, \widehat{\sigma}), \quad (n, \lambda) = \delta^{-1}(\widehat{n}, \widehat{\lambda}), \tag{31}$$

where $\epsilon \ll 1$, $\delta \ll 1$ we can repeat the above procedure. When $\epsilon = o(\delta)$ we obtain

$$\tilde{\nabla}^2 \psi'_{0t} + 2\widehat{\Omega} v'_{1z} = v_A^2 \tilde{\nabla}^2 \phi'_{0z} \tag{32}$$

$$v_{1t} - (2\widehat{\Omega} + \widehat{\sigma} + V'(x))\psi_{0z} = v_A^2 b_{1z} - v_A^2 B'(x)\phi_{0z} \tag{33}$$

$$\phi_{0t} = \psi_{0z} \tag{34}$$

$$b_{1t} - B'(x)\psi_{0z} = v_{1z} - (\widehat{\sigma} + V'(x))\phi_{0z} \tag{35}$$

$$\widehat{\nu} V'(x) = \overline{\psi_0 v_{1z}} - v_A^2 \overline{\phi_0 b_{1z}} \tag{36}$$

$$\widehat{\eta} B'(x) = \overline{\psi_0 b_{1z}} - \overline{\phi_0 v_{1z}} \tag{37}$$

In these equations $\tilde{\nabla} \equiv (\partial_x, 0, \partial_z)$, where $\tilde{x} \equiv x/\delta$ is a fast scale. Hence full spatial dependence is retained.

# Single channel mode

With $\partial_X \overline{v}_{00} = \partial_X \overline{b}_{00} \equiv 0$ the reduced equations admit exponentially growing solutions of the form (Goodman and Xu, 1994)

$$\begin{aligned} \psi_{00} &= \Psi_0(t)\cos\widehat{n}z, \quad v_{11} &= V_0(t)\sin\widehat{n}z, \\ \phi_{00} &= \Phi_0(t)\sin\widehat{n}z, \quad b_{11} &= B_0(t)\cos\widehat{n}z, \end{aligned} \tag{38}$$

However, within the theory an initial state with $\widehat{n} = \widehat{n}_{\max}$ and $\partial_X \overline{v}_{00} = \partial_X \overline{b}_{00} = 0$ develops nonzero $\partial_X \overline{v}_{00}$, $\partial_X \overline{b}_{00}$, resulting in a transition from exponential growth to algebraic growth in time.

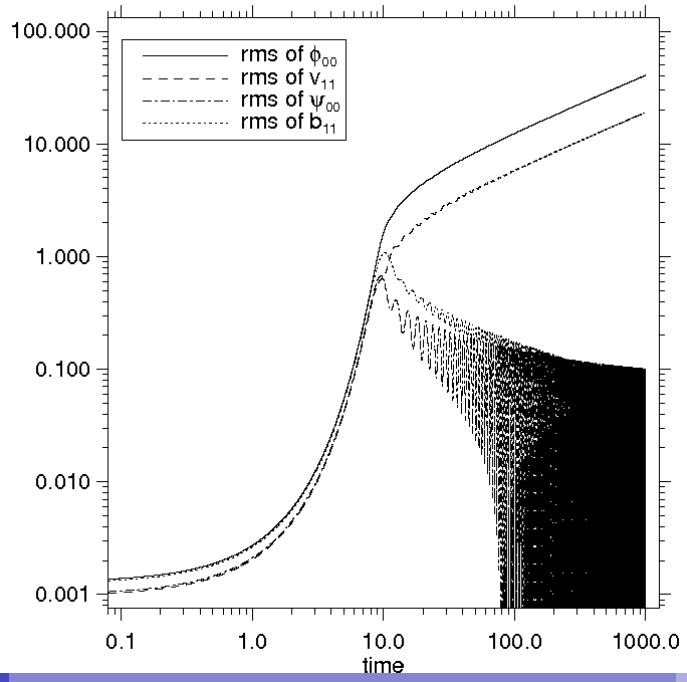

# Single channel mode

Despite unbounded algebraic growth and decay in the single channel mode $\langle \partial_X v_{00} \rangle_V \to \partial_X \overline{v}_{00}$ as $t \to \infty$. Thus $\langle \partial_X v_{00} \rangle_V$ reaches a **stable** saturated state, as does the transport of angular momentum.

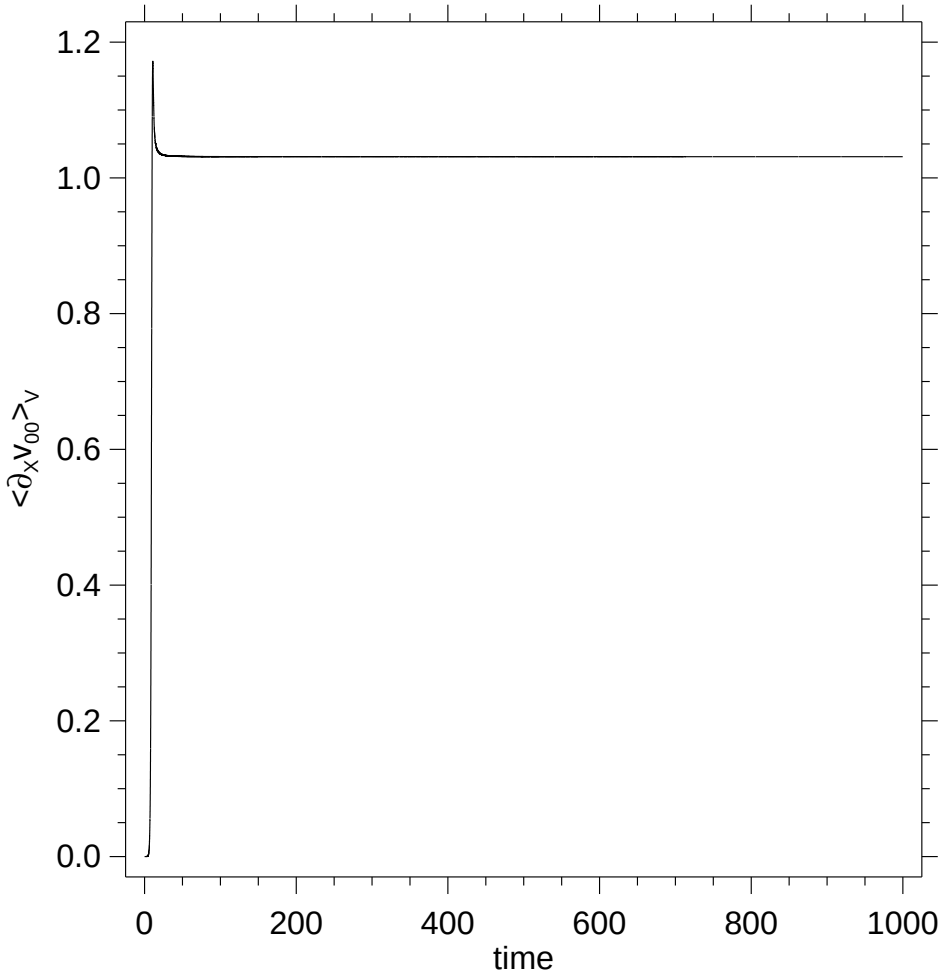

# Multiple channel modes

We select a uniform distribution of wavelengths in $z$ spanning a range of modes from $\widehat{n} \leq 4/(N_z L)$ to twice the cutoff wavelength $L_{\rm cutoff} \equiv 2\pi/\sqrt{\widehat{\chi}} = \sqrt{5}L/4$. The mode amplitudes are sampled from a uniform distribution with upper bound $10^{-4}$ and exhibit **coarsening**.

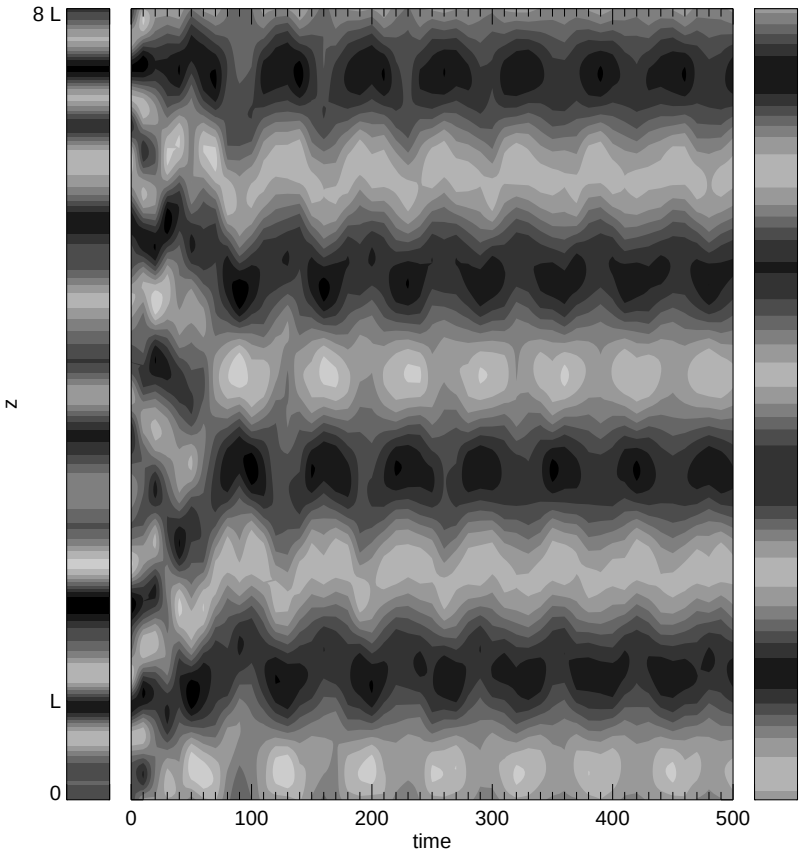


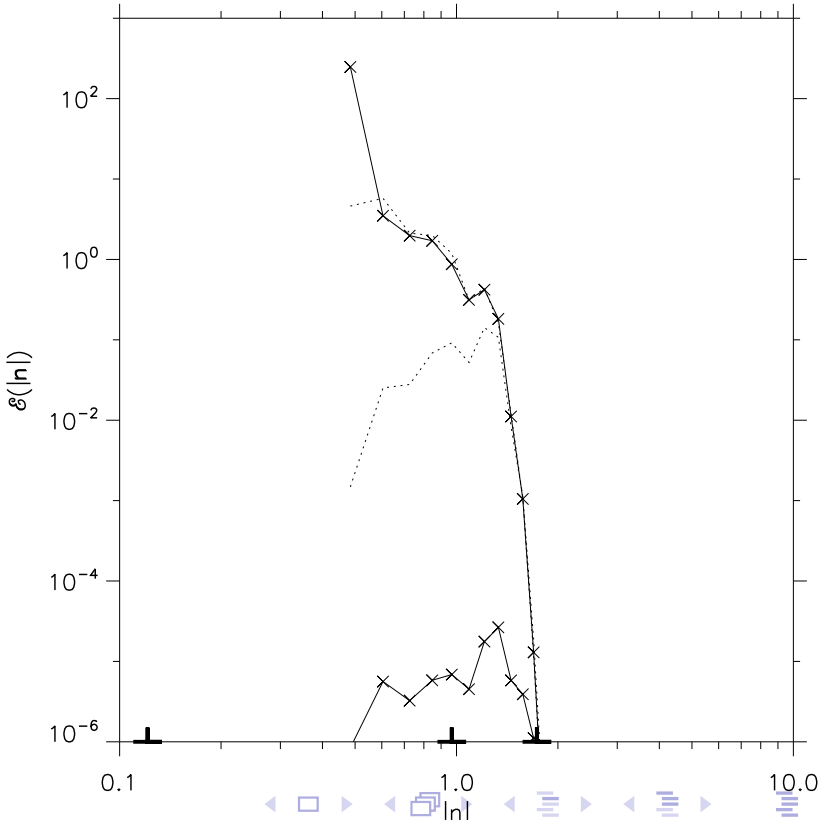

# Multiple channel modes

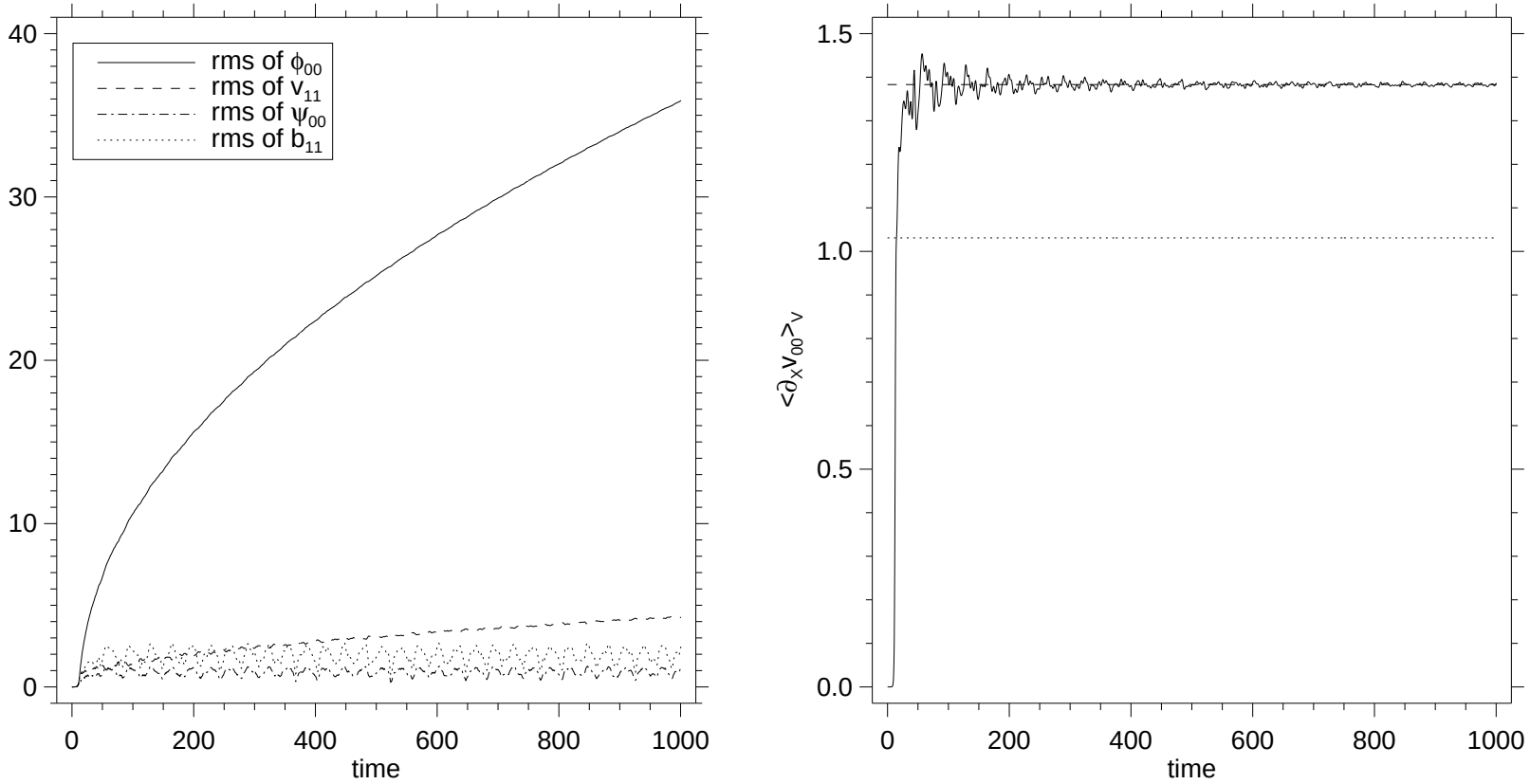


Evolution of (a) the rms fields and (b) $\langle \partial_X \overline{v}_{00} \rangle_V$. The results with $\widehat{n}_{\max}$ (dotted) and the smallest vertical wavenumber permitted $\widehat{n}_{\mathrm{eff}}$ (dashed) are also shown.

# Multiple channel modes

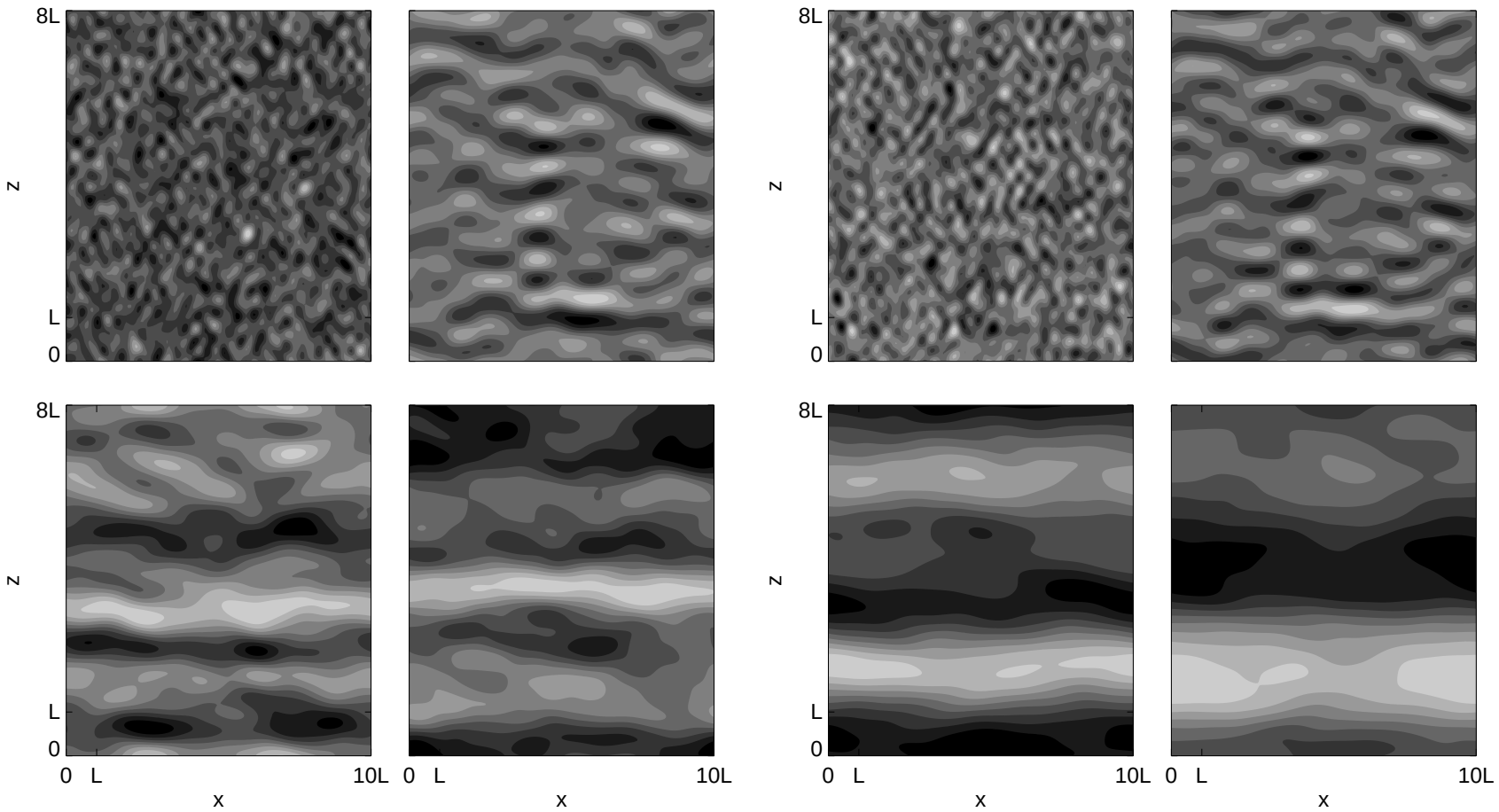


Evolution of (a) $\psi_{00}/\langle\psi_{00}^2\rangle_V^{1/2}$ and (b) $\phi_{00}/\langle\phi_{00}^2\rangle_V^{1/2}$ at $t = 0, 10, 350, 1000$.

# Multiple channel modes

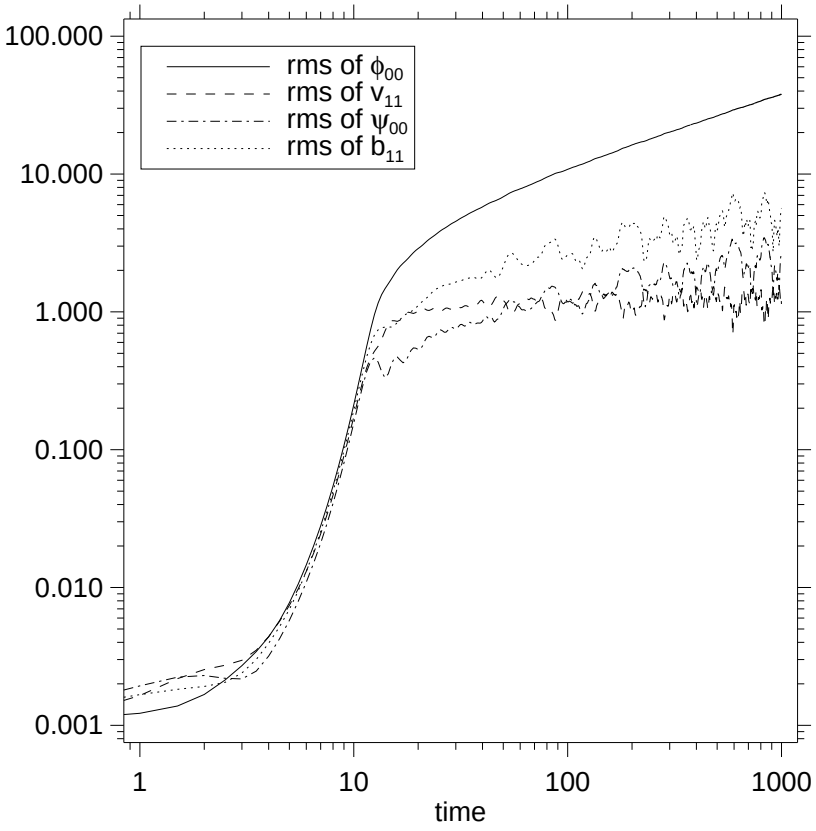


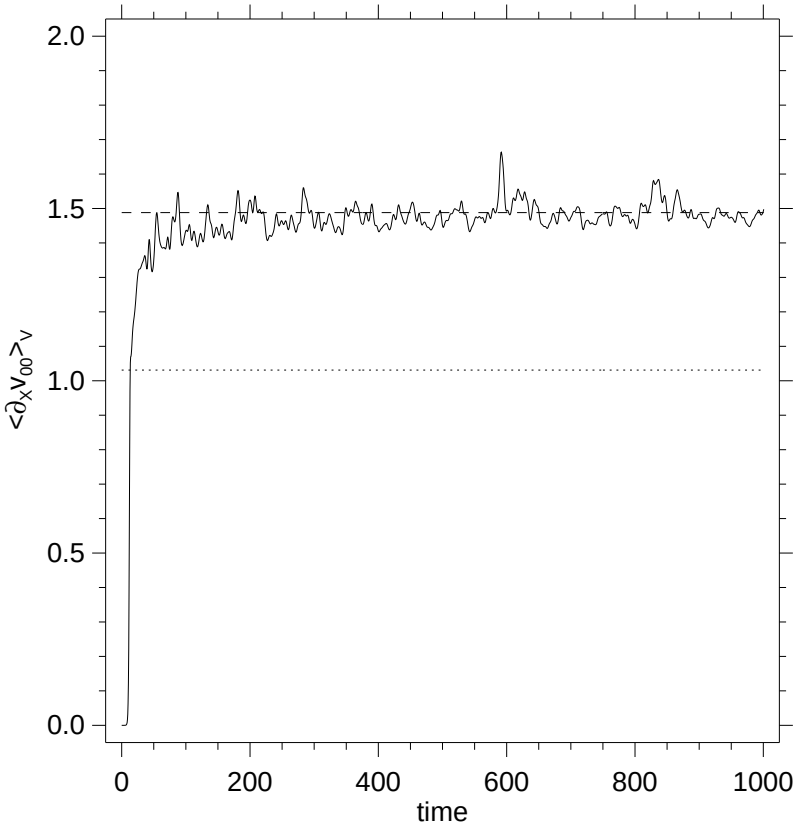


Evolution of an $x$-dependent initial Multiple Mode state

# Multiple channel modes: coarsening

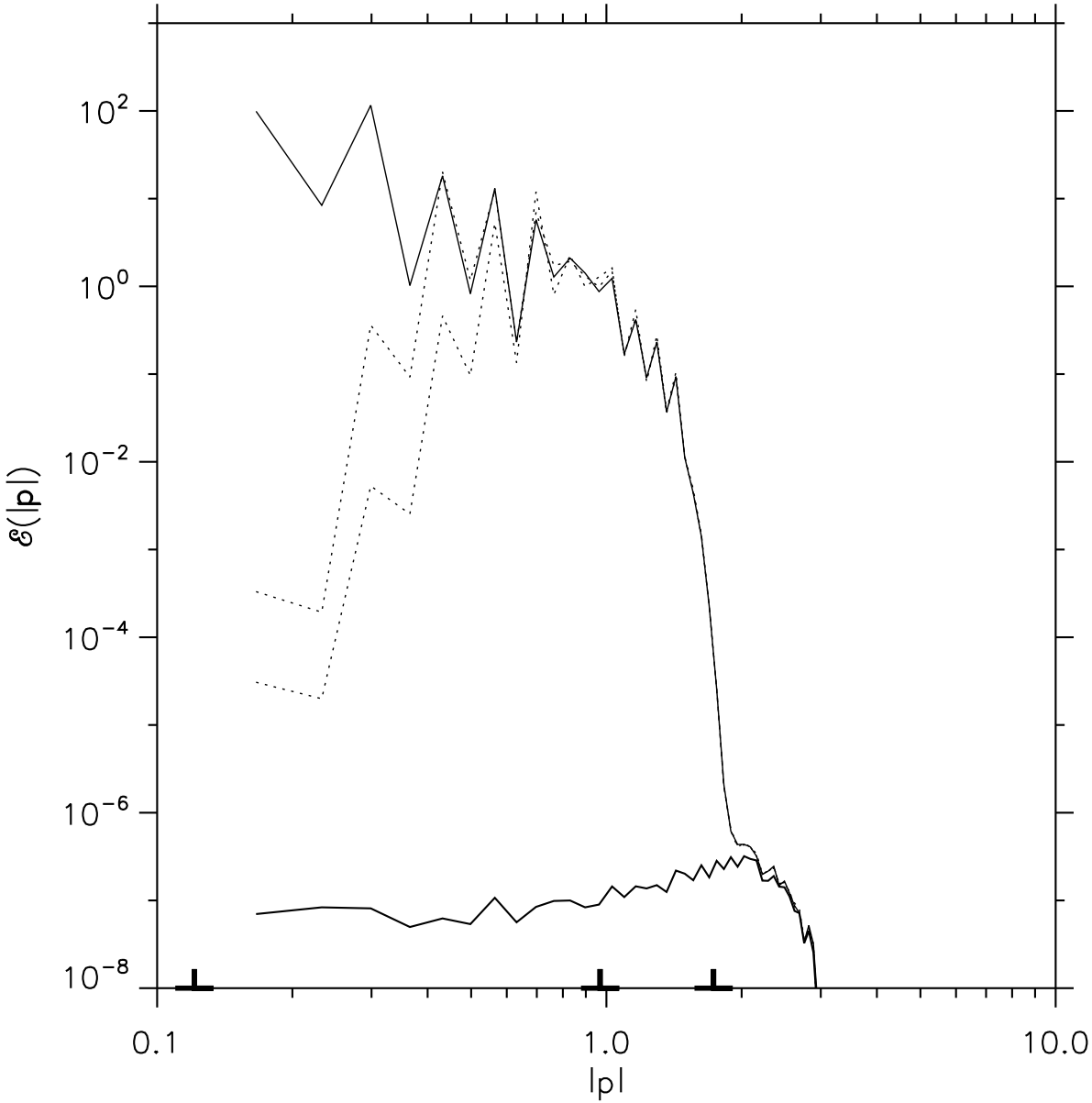

# Subdominant Dissipation

When explicit (ohmic) dissipation $\epsilon_\eta \nabla^2$ is retained (with $\epsilon_\eta = 0.01$) the algebraic growth of the fluctuations also saturates

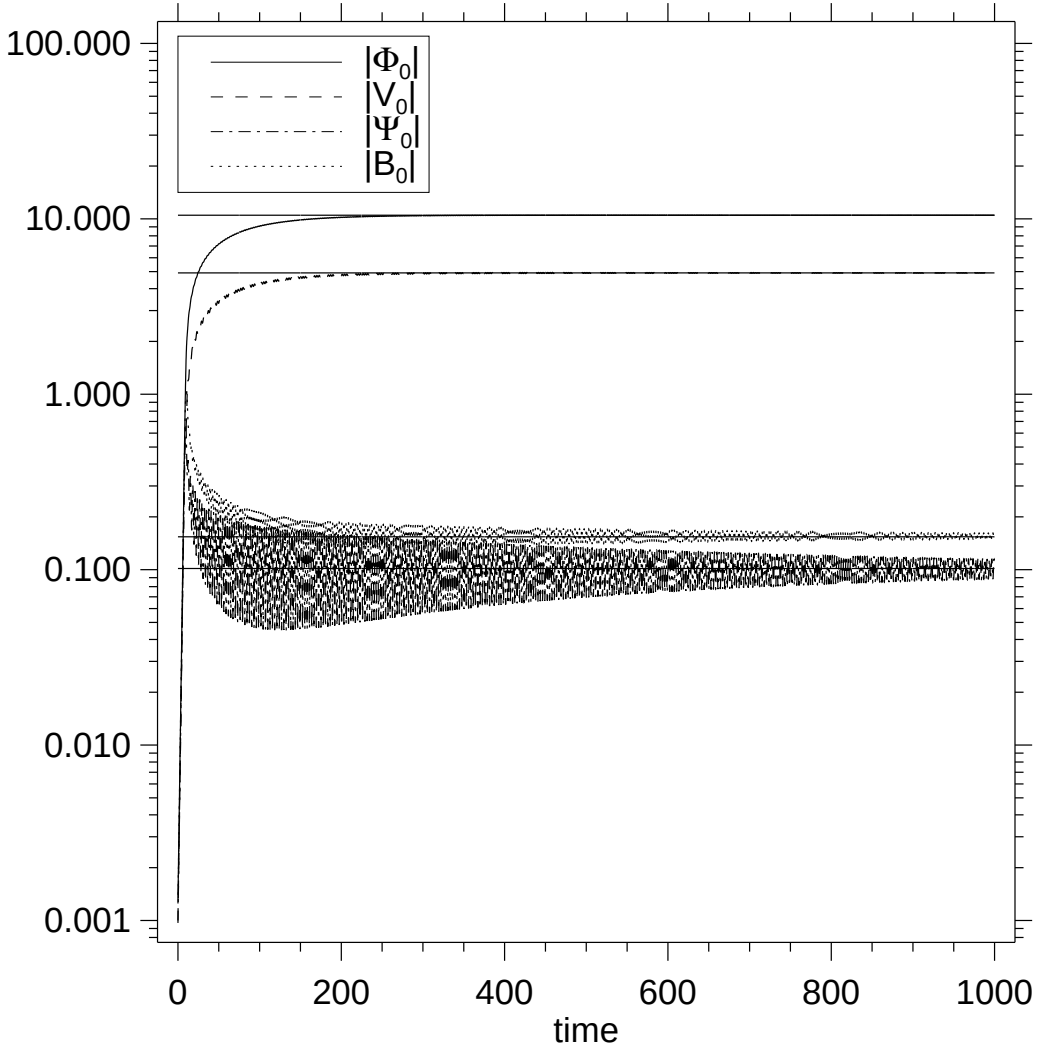

# Theory

When the nonlinear terms $\partial_X \overline{v}_{00}$, $\partial_X \overline{b}_{00} = 0$ are ignored the solution of the reduced equations is

$$(\Psi_0(t), V_0(t), \Phi_0(t), B_0(t)) \equiv \left(1, -2\frac{\widehat{n}_{\max}}{\widehat{\sigma}}, -\widehat{n}_{\max}, 2\frac{\widehat{n}_{\max}^2}{\widehat{\sigma}}\right) e^{\lambda_{\max} t}.$$

This solution is in fact an exact solution of the nonlinear fluctuating equations as obtained by Goodman and Xu (1994). But when these terms are included the exponential growth becomes algebraic

$$\begin{aligned} \psi_{00} &= (\Psi_1 t^{-\alpha} + \Psi_2 \cos\omega t)\cos(\widehat{n}z) \\ v_{11} &= (V_1 t^{\alpha} + V_2 \sin\omega t)\sin(\widehat{n}z) \\ \phi_{00} &= (\Phi_1 t^{\beta} + \Phi_2 \sin\omega t)\sin(\widehat{n}z) \\ b_{11} &= (B_1 t^{-\beta} + B_2 \cos\omega t)\cos(\widehat{n}z), \end{aligned} \tag{39}$$

where $\alpha > 0$, $\beta > 0$.

# Theory

One finds that $\alpha = \beta = 1/2$ with

$$(\Psi_1, V_1, \Phi_1, B_1) \equiv \left(1, \frac{\widehat{n}^3 v_A^2}{\widehat{\Omega}}, -2\widehat{n}, -\frac{2\widehat{\Omega}}{v_A^2}\right)\Psi_1 \tag{40}$$

$$(\Psi_2, V_2, \Phi_2, B_2) \equiv \left(1, -\frac{2\widehat{n}\widehat{\Omega}}{|\omega|}, -\frac{\widehat{n}}{|\omega|}, \frac{\widehat{n}^2}{2\widehat{\Omega}}\right)\Psi_2, \tag{41}$$

together with the necessary conditions

$$\partial_X \overline{v}_{00} = -\widehat{\sigma} - \frac{v_A^2 \widehat{n}^2}{2\widehat{\Omega}}, \qquad \partial_X \overline{b}_{00} = 0, \tag{42}$$

and

$$\omega = \sqrt{4\widehat{\Omega}^2 + \widehat{n}^2 v_A^2}. \tag{43}$$

Substituting the general form of the solutions (39) into the turbulent stress balance (Eq. (21) with volume averaging) and using the form of the eigensolutions (40), (41) yields

# Theory

$$\widehat{\nu}\,\langle \partial_X v_{00}\rangle_V = \frac{\widehat{n}^2\omega^2}{2\widehat{\Omega}}\Psi_1^2 - \frac{\widehat{n}^2\omega}{8\widehat{\Omega}}\sin 2\omega t\Psi_2^2. \tag{44}$$

It is remarkable that this expression does not contain secular terms proportional to $t^{1/2}\cos\omega t$, $t^{-1/2}\sin\omega t$ or indeed $t$, and hence saturates despite the algebraic growth of the contributing fields (cf. Landau damping). The mean component arises from products of the terms $\Phi_1 t^{\frac{1}{2}}$, $V_1 t^{\frac{1}{2}}$ and $\Psi_1 t^{-\frac{1}{2}}$, $B_1 t^{-\frac{1}{2}}$, while the oscillatory component is a consequence of the terms $(\Psi_2, V_2, \Phi_2, B_2)$. On time-averaging this result and comparing with Eq. (42) we obtain finally

$$\Psi_1^2 = \frac{2\widehat{\nu}\widehat{\Omega}}{\widehat{n}^2\omega^2}\partial_X \overline{v}_{00} = \frac{\widehat{\nu}v_A^2}{\widehat{n}^2\omega^2}\left(-\frac{2\widehat{\Omega}\widehat{\sigma}}{v_A^2} - \widehat{n}^2\right). \tag{45}$$

# Theory

We can numerically verify the relation (43) by measuring $\omega$ for a range of values of $\widehat{\Omega}$, with the remaining parameters fixed.

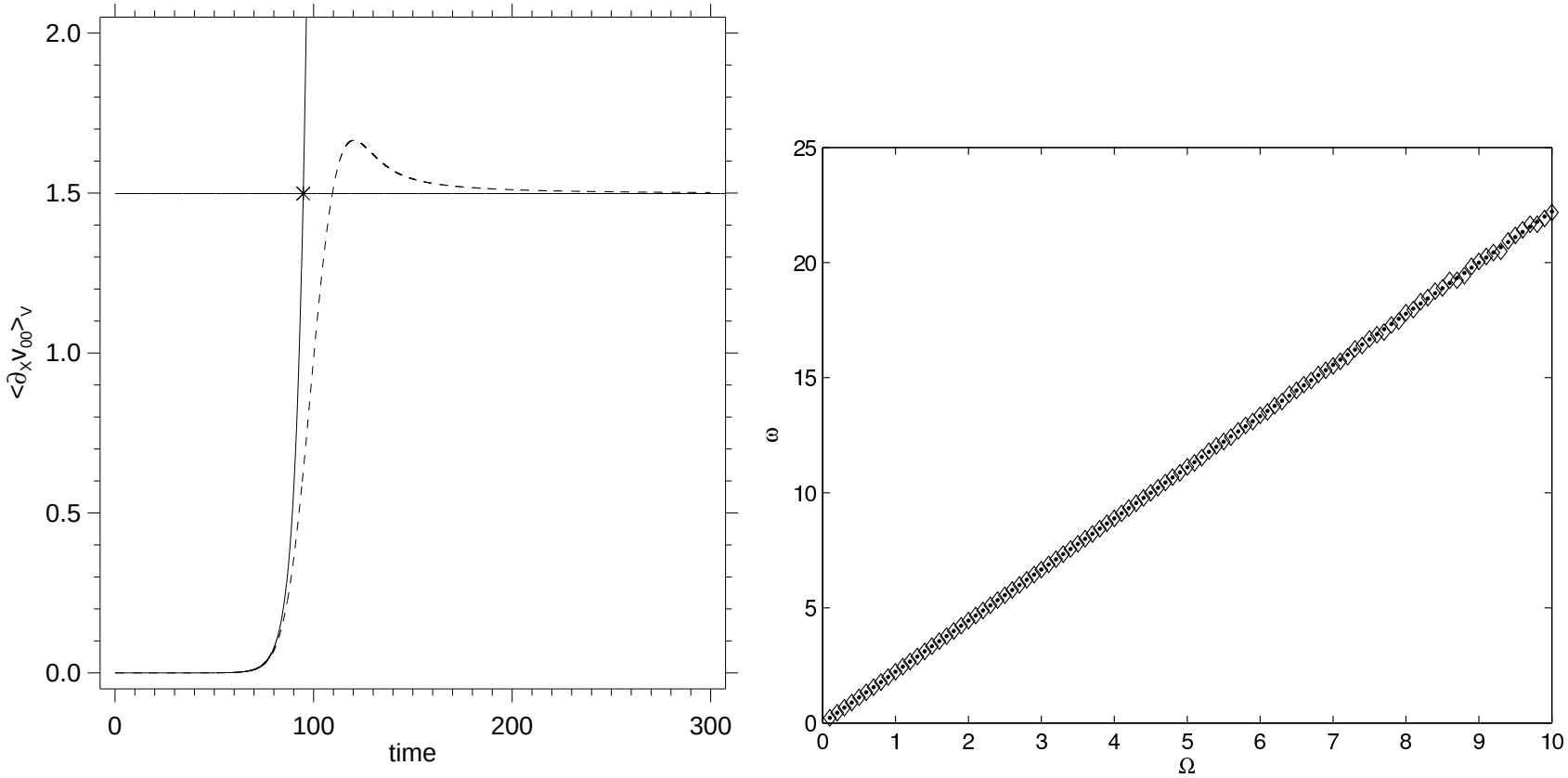


(a) Back-reaction saturates the growth of $\langle \partial_X v_{00} \rangle_V$, (b) $\omega(\widehat{\Omega})$

# Summary

- Simple scaling suffices to characterize one-parameter family of self-consistent equilibrated states
  - Strong modification of the background shear that feeds the MRI
  - Equilibration ultimately determined by ohmic + viscous dissipation
- Comparison with shearing-box simulations (BH 1991, HGB 1995, Sano et al 1998)
  - With resistive effects included but viscosity excluded no saturation occurs for $\Lambda > 1$. Our theory indicates viscosity plays an important role in this regime (Fromang & Papaloizou 2007)
  - Saturated MRI speed is $O(1)$, but the effective viscosity is $O(\epsilon)$
  - Simulations (Hawley & Balbus 1991) show tendency towards solid body rotation and increased wavelength of MRI. This is also consistent with the theory

# Relation to astrophysics

- We have a theory that is valid in an asymptotic regime relevant to astrophysical accretion disks
- This regime is not accessible to fully resolved simulations
- It is expected that accretion disks are in fact turbulent. In this case it may be possible to take $\eta$ and $\nu$ in the theory to be the turbulent diffusion coefficients

It would be useful to extend the theory to

- Cylindrical geometries to overcome degeneracy in direction of angular momentum transport
- Include compressibility

Details in:


- E. Knobloch and K. Julien, Phys. Fluids 17, 094106 (2005);
- K. Julien and E. Knobloch, in Stellar Fluid Dynamics and Numerical Simulations: From the Sun to Neutron Stars, M. Rieutord and B. Dubrulle (eds), EAS Publication Series 21 (2006);
- K. Julien and E. Knobloch, J. Math. Phys. 48, 065405 (2007);
- B. Jamroz, K. Julien and E. Knobloch, Phys. Scr. T132, 014027 (2008a);
- B. Jamroz, K. Julien and E. Knobloch, AN 329, 675 (2008b).